

THE PHYSICOCHEMICAL PROPERTIES OF SFE FIRE SUPPRESSANT ATMOSPHERES IN TOXICITY vs. FIRE EXTINGUISHMENT TESTS: Implications for aerosol deposition and toxicity.

Edgar C. Kimmel*[†], Eldon A. Smith*, James E. Reboulet* and Robert L. Carpenter^{oo}

^{oo} Naval Medical Research Institute Detachment (Toxicology) (NMRI/TD)

Bldg. 433, Area B, Wright-Patterson AFB, OH 45433-7903, * Geo-Centers, Inc.

[†] To whom correspondence should be addressed at NMRI/TD

ABSTRACT

The physical and chemical properties of SFE (a dry powder) fire extinguishant atmospheres generated to assess inhalation toxicity in a whole-body exposure system were compared with those generated in facilities used to evaluate fire extinguishment efficacy. The purpose was to establish a basis for extrapolation of laboratory toxicity testing data to field conditions. Nominal concentrations of 50 and 80 g/m³ in both systems were examined. Mass concentration and concentration decay of the aerosol component, aerosol size distribution and particle growth, and concentration profile of CO and CO₂, the major gaseous components of SFE atmospheres, were determined. The mass concentration of SFE aerosols in the large system was 1.5 times greater than that in the exposure chamber. Aerosol concentration in both systems decayed exponentially at comparable rates. Hygroscopic growth of the particles was greater and more rapid in the large system. Gas concentrations in the larger test system also were greater by a factor of 1.5. However, in this system gas concentrations also underwent exponential decay whereas gas concentrations in the exposure chambers were steady-state over the 1 hour test periods. Laboratory exposures at the higher target load concentrations produced pulmonary edema and elevated COHb in rats. Theoretical, mathematical expressions characterizing CO₂ induced hypercapnea in humans, and the potential effects of elevated ventilation on particle deposition and COHb formation were derived as a basis for comparison of the potential toxicity of the atmospheres.

INTRODUCTION

A comparison of the physicochemical properties of atmospheres of Spectronix Fire Extinguishant (SFE), a dry powder aerosol extinguishant, generated at two nominal concentrations (50 and 80 g/m³) in either a 0.7 m³ inhalation toxicology exposure system¹ or in a 56 m³ fire extinguishment testing system² was conducted recently as part of a program to evaluate potential Halon replacements. Generation and delivery of the SFE atmospheres in the larger system simulated, more closely, SFE fire-fighting deployment conditions. Although the latter test scenario had been investigated extensively for fire extinguishment efficacy, the aerosol component of the atmosphere(s) had not been characterized. Fundamental differences in aerosol concentration and size distribution, major gaseous component (CO & CO₂) concentrations, constituent proportion, and dynamic behavior of the various components were found between atmospheres generated at identical nominal concentrations in the two systems. In addition to aerosol characterization in the large system, the purpose of the investigation was to facilitate extrapolation of SFE inhalation toxicity data (see companion manuscripts - this report) for assessment of the potential health risk of SFE atmospheres as deployed for fire extinguishment. Operational safety considerations, and the need to isolate SFE specific toxicity from untoward thermal and pressure artifacts from SFE generation proscribed modification of the inhalation exposure system to eliminate these fundamental differences between the atmospheres.

Comparison of the aerosol concentration and size distribution (including particle growth), as well as comparison of the gaseous component concentration differences between the atmospheres, was complicated by the variable proportionality and dynamic behavior of the atmospheric constituents. The variable rates of change of mass concentration and constituent proportion confounded a relatively straight-forward extrapolation of toxicity data based on markers of exposure alone. Atmospheric component alteration of normal respiratory physiology also was a confounding factor in the atmosphere comparison/extrapolation process. Consequently a series of theoretical calculations of component effects on respiration in humans were developed and were used to form the basis for an evaluation of potential toxicity of SFE due to aerosol deposition and COHb formation. A 3-dimensional graphical approach to data analysis was used for simultaneous illustration of the atmospheric component(s) dynamic behavior and physiological interaction to facilitate comparison of the potential toxicity of the various SFE atmospheres.

1. at Naval Medical Research Institute Detachment (Toxicology)
2. at Naval Research Laboratory/Chesapeake Bay Detachment

METHODS AND MATERIALS

Test Material

SFE (formulation A) was obtained from Spectrex, Inc., the U.S. subsidiary of Spectronix, Ltd., Israel. The composition of SFE is proprietary.

Atmosphere Generation

In both test systems the SFE atmospheres were generated pyrotechnically by electrothermal, resistance heating of bulk material to 500 °C. Two nominal concentrations of 50 and 80 g/m³ (mass of material pyrolyzed per unit test chamber volume) were investigated in each system. In the fire extinguishment (56 m³) system the SFE was ignited directly within the chamber volume. In the inhalation exposure (0.7 m³) system SFE was ignited in a separate generator to dissipate the ignition pressure and thermal pulses prior to delivery of the atmosphere to the chamber. The atmosphere was transported from the generator assembly to the exposure chamber via 2.5 m of wide bore (7.62 cm dia.) aluminum duct at low velocity to minimize aerosol loss.

Test/Exposure System

Because SFE generation was not continuous the 0.7 m³ whole-body inhalation exposure chamber was operated in a static mode except during SFE pyrolysis (15 sec) and transport to the chamber (45 sec) when push/pull 30 L/min flow, at an initial 5 in. H₂O subambient pressure, was passed through the generator - chamber assembly. Immediately after delivery of the atmosphere the chamber inlet and exhaust ports were sealed via electropneumatic valves. The chamber was operated as a sealed (air tight) system. The 56 m³ chamber was a cinder block building with a blast-door ceiling and was not considered a sealed system. Each test period was 1hi, and the number of trials were as follows:

0.7 m³ at 50 g/m³ (0.7-50) - 3
0.7 m³ at 80 g/m³ (0.7-80) - 4
56 m³ at 50 g/m³ (56-50) - 3
56 m³ at 80 g/m³ (56-80) - 2.

Aerosol Analysis

Aerosol mass concentration was determined by gravimetric analysis of glass fiber filter samples. Filter holders were located within the large chamber at the terminus of individual sample lines. Aerosol size distribution (mass median aerodynamic diameter - MMAD and geometric standard deviation - σ) was determined by gravimetric analysis of multi-stage [8], multijet cascade impactor (Intox Products) samples. Size distribution shifts (particle growth) were determined by laser optic time of flight analysis of individual particles (3300B - Aerodynamic Particle Sizer, TSI, Inc.) Filter and impactor samples were taken at 1 or 1.5, 15, 30 and 60 min.

Electrostatic precipitator (02-1500, Intox Products) samples were collected for examination of particle morphology by scanning and transmission electron microscopy (SEM & TEM). Multistage cyclone samples were collected for Braunuer-Emmitt-Teller (BET) particle specific surface area (SSA), ultrapycnometric particle density, and X-ray defraction particle composition analyses.

Gas Analysis

Gas chromatography was used for analysis of CO, grab samples in the 56 m³ chamber (3). CO concentration in the 56 m³ chamber was monitored continuously by flowing non-dispersive, wavelength specific infrared (NDIR) spectroscopy (Enviromax 3000, Liston Scientific). Electro-chemical analysis of O₂ was continuous for the 56 m³ chamber (Enviromax 3000) and on a grab sample basis for the 0.7 m³ chamber (362RA, Teledyne Analytical Instruments). In the 0.7 m³ chamber both CO, and CO concentrations were determined by NDIR spectroscopy (865, Beckman Industries).

RESULTS

Aerosol Concentration, Size Distribution, Growth, and Morphology

Actual (non-nominal) initial and final aerosol concentrations for the various SFE atmospheres are shown in Table 1. Because of the non-continuous generation of SFE atmospheres and static operation of the chambers the aerosol concentrations in the test chambers underwent exponential decay due to gravitational settling (Figure 1). Aerosol MMAD's and σ_g 's are shown in Table 1. Aerosol particle growth patterns are shown in Figure 2. SEM and TEM showed that in the 0.7 m³ chamber where conditions were relatively dry (30 % RH) the aerosol particles were single and agglomerates of cuboidal crystals. In the moist conditions (RH 90+ %) under which analyses in the 56 m³ chamber were performed both single and agglomerate particles showed surface remodeling with rounded edges and meniscus formation between individual particles in the agglomerates (electronmicrographs not presented). Energy dispersive X-ray analysis indicated that the SFE particles were KCl. BET analysis indicated particle SSA was 2.74 m²/g which was comparable to a predicted SSA of 2.08 m²/g. Pycnometry indicated SFE particle density was 2.23 g/cm³ which was slightly higher than the bulk density of KCl (1.98 g/m³).

Gas Concentrations

Initial and final CO, CO₂, and O₂ concentrations are shown in Table 2. CO and CO₂ concentration in the 56 m³ chamber decayed exponentially due to diffusion from this non-sealed chamber (Figures 3,4). Initial values for CO in the 56 m³ chamber were extrapolated from 20 minute time point due to a sampling error. Values for the extrapolated data were derived from the CO₂ decay curve using Graham's law for diffusion coefficient ratios.

DISCUSSION

Based on recent International Commission on Radiation Protection curves, SFE aerosol particle growth would result in a moderate increase in total lung (TL) particle deposition, with larger increases in naso-oro-pharyngeal (NP) and tracheobronchial (TB) regional deposition. The greatest changes in fractional deposition would be decreased pulmonary region (P) deposition (Table 3). Because of varying clearance rates from these compartments changes in regional, particularly P region deposition, would be of greater concern were SFE aerosol particles not so highly soluble. As a consequence, changes in TL deposition were considered the most relevant. Because TL deposition changes were moderate, differences in particle growth rate between the various SFE atmospheres were considered relatively insignificant. TL deposition rates for the SFE atmospheres at peak, steady-state aerosol concentrations are given in Table 4. However as a basis for comparison of the potential aerosol toxicity between the atmospheres these data are limited because they do not account for simultaneous changes in aerosol concentration and CO₂ induced hypercapnea. Although there are numerous untoward effects that could be associated with CO₂ inhalation (ie disturbance in acid-base homeostasis) only effects on minute ventilation (V_e) are considered here.

Stimulation of respiration by breathing CO₂ has been shown to be more directly related to alveolar partial pressure of CO₂ (P_{Aco₂}) than to fractional concentration of CO₂ in the respiratory gas. Although directly related to atmospheric CO₂ concentration P_{Aco₂} is also influenced by ventilatory and metabolic factors. Existing quantitative descriptions of steady-state gas exchange and V_e as a function of P_{Aco₂}, inspired CO₂, and O₂ concentrations, respiratory quotient and other physiological parameters were not amenable for calculation of atmospheric CO₂ induced hypercapnea under the dynamic conditions observed. Consequently, based on a review of the literature a series of first approximation and empirical equations were formulated to describe CO₂ induced hypercapnea in other than steady-state conditions.

Data from the literature relating PAco₂ to atmospheric CO₂ (Figure 5) were fitted ($r^2 = 0.99199$) to the following equation:

$$PAco_2 = 33.8991 + 0.00149x^{0.9245} \quad \{1\}$$

where $x = CO_2$ (ppm), 33.8991 normal PAco₂ (mmHg) not corrected for BTPS (ie $40 \times 0.863 = 34.52$), 0.00149 0.00152 (2 times 0.00076, the conversion factor for ppm CO₂ to mmHg CO₂, - factor of 2 accounts for equilibrium between blood and alveoli assuming no metabolic CO₂), and 0.9245 \cong the correction factor for barometric pressure less water vapor pressure at 37 °C = 0.9382. Non-linear regression of data from the literature relating PAco₂ and Ve yielded a sigmoidal curve ($r^2 = 0.99283$ - Figure 6):

$$Ve = 0.21387 + 6.202898 / (1 + \exp(-(x - 40.7476) / 8.5355)) \quad \{2\}$$

where $x = PAco_2$.

Equation 1 and 2 were combined and with additional data from the literature directly relating CO₂ concentration to Ve were subject to a second non-linear regression yielding the following empirical sigmoidal curve ($r^2 = 0.99892$ - Figure 7):

$$Ve = -0.7256 + 63.9715 / (1 + \exp(-(x - 58949.29) / 14807.62)) \quad \{3\}$$

where $x = CO_2$ (ppm).

The sigmoidal shape of the curves was expected, with asymptotic limits explicable by physiological correlates. Equation 3 was combined with the regressions (all $r^2 \geq 0.998$ - see Figure 3) describing CO₂ concentration exponential decay in each of the SFE atmospheres to obtain a series of curves describing the course of CO₂ induced hypercapnea for the 1 hr test period, assuming a baseline Ve of 7 L/min (Figure 8). Assuming a 1:1 correlation between change in Ve and deposition these curves yielded a series of curves describing fractional increase in aerosol deposition due to hypercapnea alone (Figure 9). A constant 0.9 fractional TL deposition and a baseline Ve = 7 L/min were assumed. These functions were combined with the aerosol concentration exponential decay functions (Figure 1) to generate a series of 3-dimensional (3-D) plots. These 3-D plots are representative of the overall increase in aerosol deposition over the course of the 1 hr exposure that combines the hypercapnea effects and aerosol dynamic behavior (Figure 10). The lowest final aerosol concentration observed (0.7 g/m³) was used to calculate a baseline deposition rate.

When plotted on an equivalent scale the relative areas of the 3-D surface maps correspond to the relative differences between the SFE atmospheres in increased particle deposition as a function of both particle concentration and ventilatory change. Since the extent of the surfaces mapped in these plots represents the range of exposure and physiological response, comparison of the surface map areas serves as an index of relative potential health risk associated with breathing these atmospheres. For a given exposure, both A Ve and Aaerosol concentration change with time; changes in deposition rate are defined by a line lying in the surface map depicted. The area of the imaginary plane "below" this "response" line (which is normal to the XY plane - parallel to Z axis) is proportional to the total increase in aerosol deposition. Total aerosol deposition change would be calculated as the integral of the response line, the area of which is bounded by the imaginary plane. The surface map (response map) show in the figures, which is a matrix composed of corresponding XYZ coordinates, is, in turn, proportional (as a function of A Z, by virtue XYZ coordinate set congruity) to the area in the imaginary plane. Thus the surface map is proportional to and representative of total change in aerosol deposition for the corresponding SFE atmosphere, given the hypercapneic A Ve assumptions.

A similar process was used to examine the differences in COHb %/min formation rate (Figure 11) using the following empirical equation from the literature:

$$\Delta\text{COHb \%} = (\text{CO} \times \text{Ve} \times \text{t}) / 2.5 \times 10^4 \quad \{4\}$$

where $\text{CO} = \text{ppm}$, $\text{Ve} = \text{L/min}$, and $\text{t} = \text{min}$.

Equation 4 was combined with the exponential decay curves (all $r^2 \geq 0.995$ - see **Figure 4**) for CO concentration in each SFE atmosphere. Curves in **Figure 8** were used to describe changes in Ve .

CONCLUSION

The use of 3-D graphics provides a useful approach to illustrate the differences in magnitude of potential inhalation toxicity of atmospheres that are chemically identical but behave dynamically with respect to concentration and vary in constituent proportionality. This approach also may be useful to illustrate the effects of an integral physiological response to one constituent in a complex atmosphere upon the potential toxicity of other components of the atmosphere, such as is the case with SFE.

References - acknowledgements/disclaimer

Much of this manuscript relies upon an extensive literature review - due to page limitations references have been omitted, but are available on request. This research was sponsored by the Navy CFC/Halon Replacement Program: NAVSEASYS COM Cadc 03V2. The Authors wish to thank HMI Charles Alva for his assistance with this project. The Authors greatly appreciate the contributions Naval Research Laboratory /Chesapeake Bay Detachment personnel (Dr. Ron Sheinson, Dr. Bruce Black & Mr. Roger Brawn) for their contributions to this effort. Opinions contained herein are those of the authors and are not to be construed as official or reflecting the view of the Department of the Navy or the Naval Service at large. Mention of commercial products or services does not constitute endorsement by the Department of the Navy or the Naval Service at Large.

TABLE 1.
SFE AEROSOL CONCENTRATION AND SIZE DISTRIBUTION

	CONCENTRATION		SIZE			
	initial	final	initial		final	
	(g/m ³)	(g/m ³)	MMAD(μm)	σg	MMAD(μm)	σg
0.7 - 50	6.3	0.7	2.8	1.66	3.3	1.69
0.7 - 80	10	0.7	3	1.67	3.2	1.7
56 - 50	10.2	1.2	2.8	1.77	4.8	1.72
56 - 80	14	1.7	2.4	1.42	4.3	2.01

TABLE 2. GAS CONCENTRATIONS

	CO ₂		CO		O ₂	
	initial (ppm)	final (ppm)	initial (ppm)	final (ppm)	initial (%)	final (%)
0.7 - 50	10,230	10,105	2,168	2,538	20.1	20.2
0.7 - 80	9,457	9,376	6,548	6,360	20.5	20.6
56 - 50	14,475	7,100	5,485	2,693	19.6	19.9
56 - 80	22,200	9,500	10,148	3,962	19.1	19.3

TABLE 3. AEROSOL GROWTH EFFECT ON PARTICLE DEPOSITION SIZE DEPOSITION FRACTION

	initial	max.	T L		N P		T B		P	
	(μm)	(μm)	initial	max.	initial	max.	initial	max.	initial	min.
0.7 - 50	2.8	3.8	0.87	0.93	0.06	0.23	0.06	0.13	0.63	0.46
0.7 - 80	3	4	0.9	0.94	0.12		0.08	0.16	0.59	0.44
56 - 50	2.8	3.8	0.87	0.95	0.08	0.24	0.07	0.21	0.63	0.37
56 - 80	2.4	6.3	0.78	0.97	0	0.33	0.05	0.37	0.66	0.23

TL = total lung region, NP = nasopharyngeal region, TB = tracheobronchial region, P = pulmonary (alveolar) region

TABLE 4. AEROSOL DEPOSITION RATES AT PEAK AEROSOL CONCENTRATIONS

	Peak Aerosol Conc. (g/m ³)	Baseline V _e (L/min)	TL Deposition Fraction *	Aerosol Deposition Rate (g/min)
0.7 - 50	6.3	7	0.9	4.41 x 10 ⁻²
0.7 - 80	10	7	0.9	7.0 x 10 ⁻²
56 - 50	10.2	7	0.9	7.14 x 10 ⁻²
56 - 80	14	7	0.9	9.8 x 10 ⁻²

* based on mean of all TL deposition fractions for observed MMADs (ventilation effects not considered)

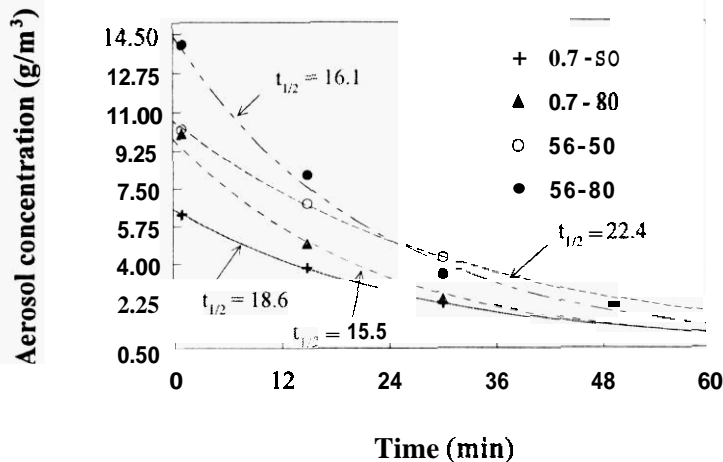


Figure 1. Exponential Decay of Aerosol Concentration

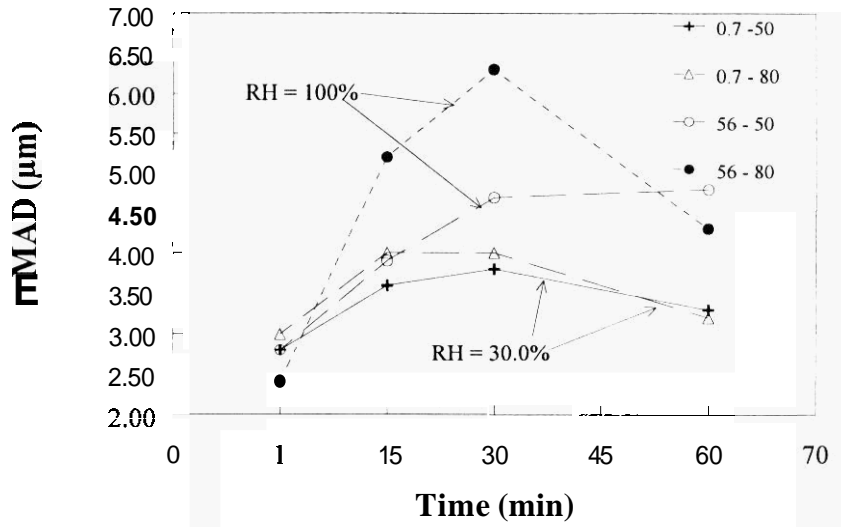


Figure 2. Aerosol Particle Growth

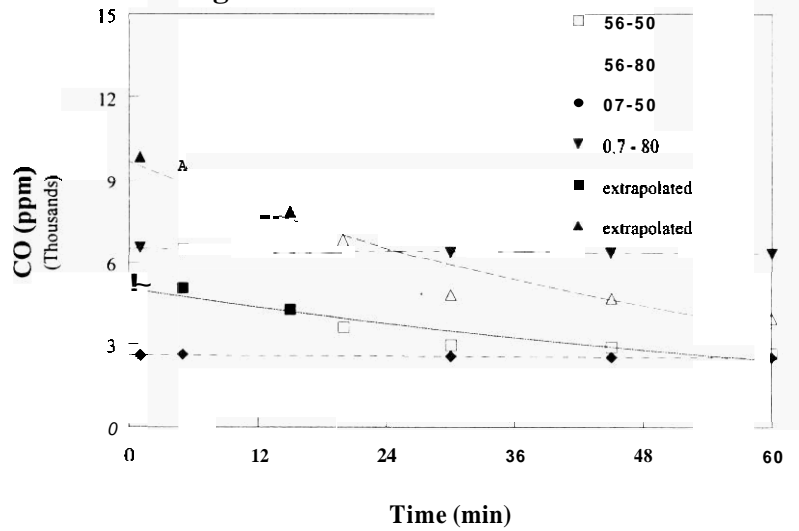


Figure 3. Exponential Decay of CO, Concentration

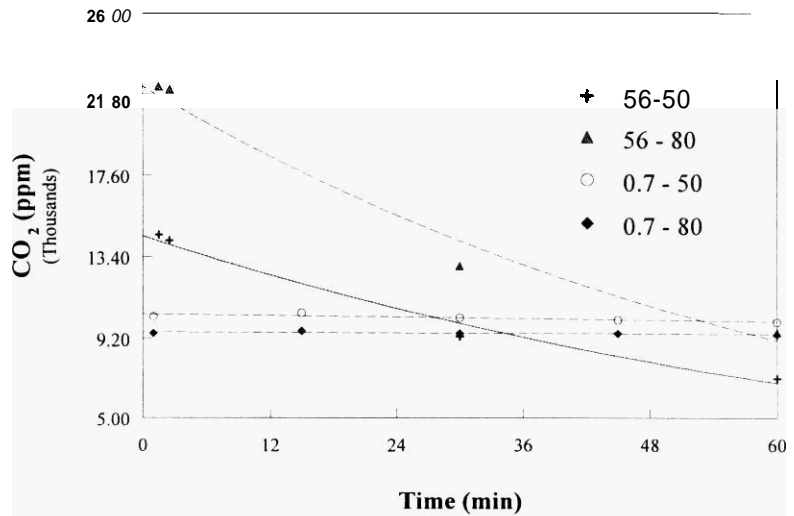


Figure 4. Exponential Decay of CO₂ Concentration

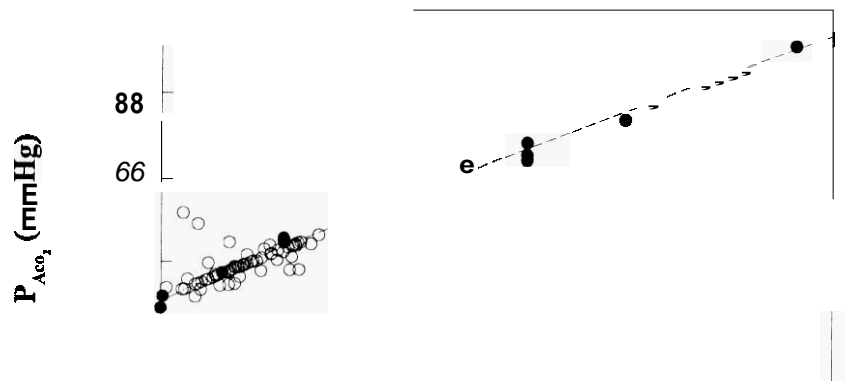


Figure 5. Alveolar CO₂ Partial Pressure vs CO₂ Concentration
 solid circles = CO, and PAco, reported directly, open circles = CO, reported and PAco, as A baseline

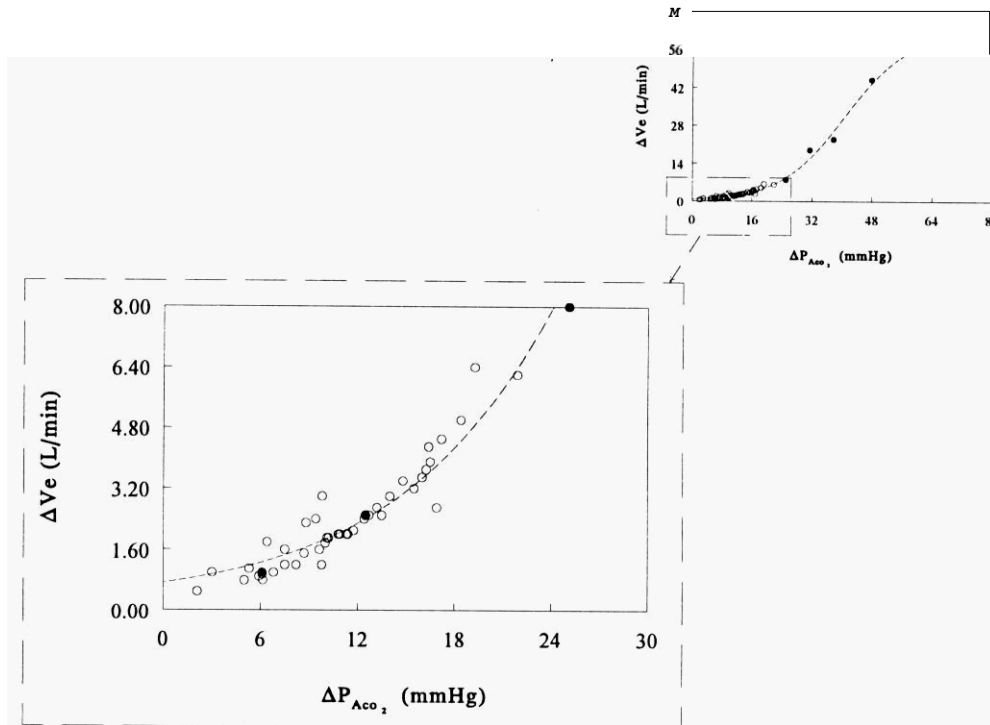


Figure 6. Hypercapnea vs Alveolar CO₂ Partial Pressure
 solid circles = Ve, CO₂, PAco, given, open circles = Ve & PAco, given CO, calculated

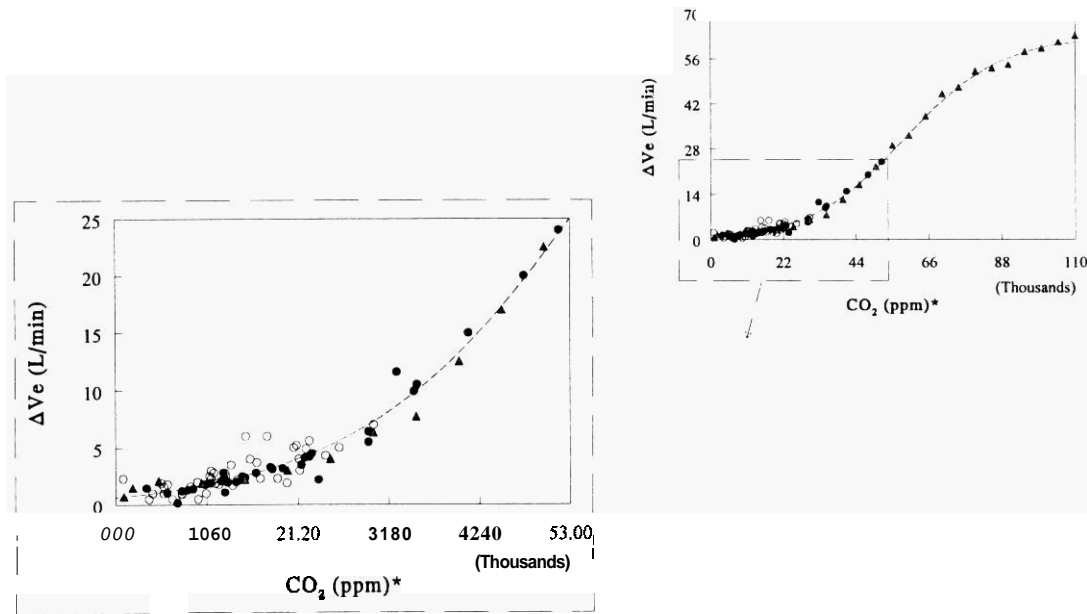
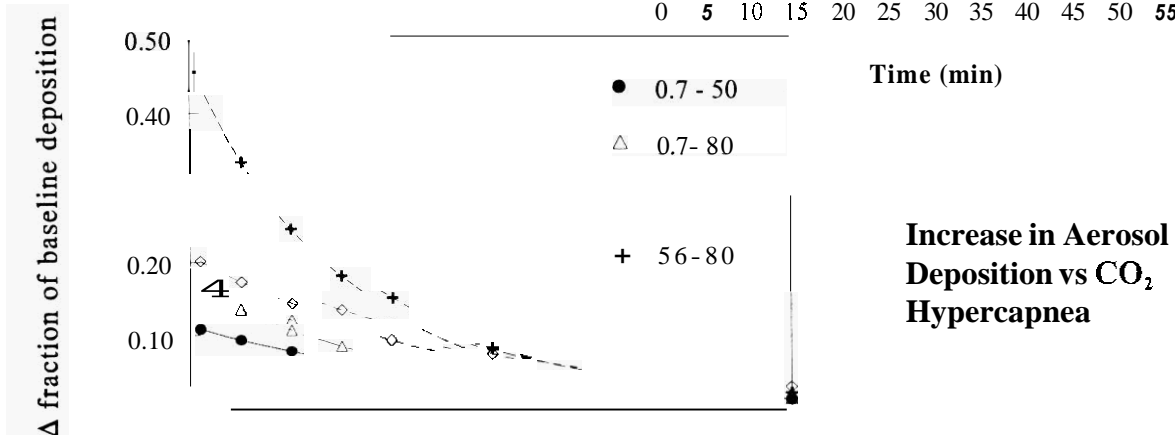
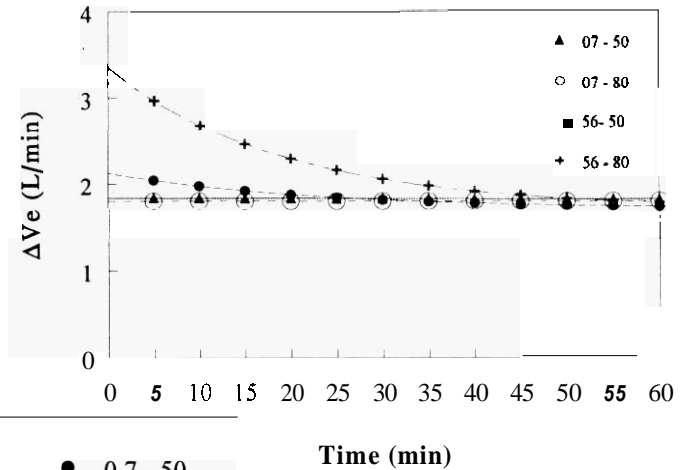


Figure 7 Hypercapnea vs Atmospheric CO₂ Concentration

* ppm based on P_{Aco}, conversion; solid circles = V_e, CO₂, P_{Aco}, given; open circles = V_e, P_{Aco}, given & CO₂ calculated; triangles = CO₂ & V_e reported directly

Figure 8. CO₂ Induced Elevation of Minute Ventilation



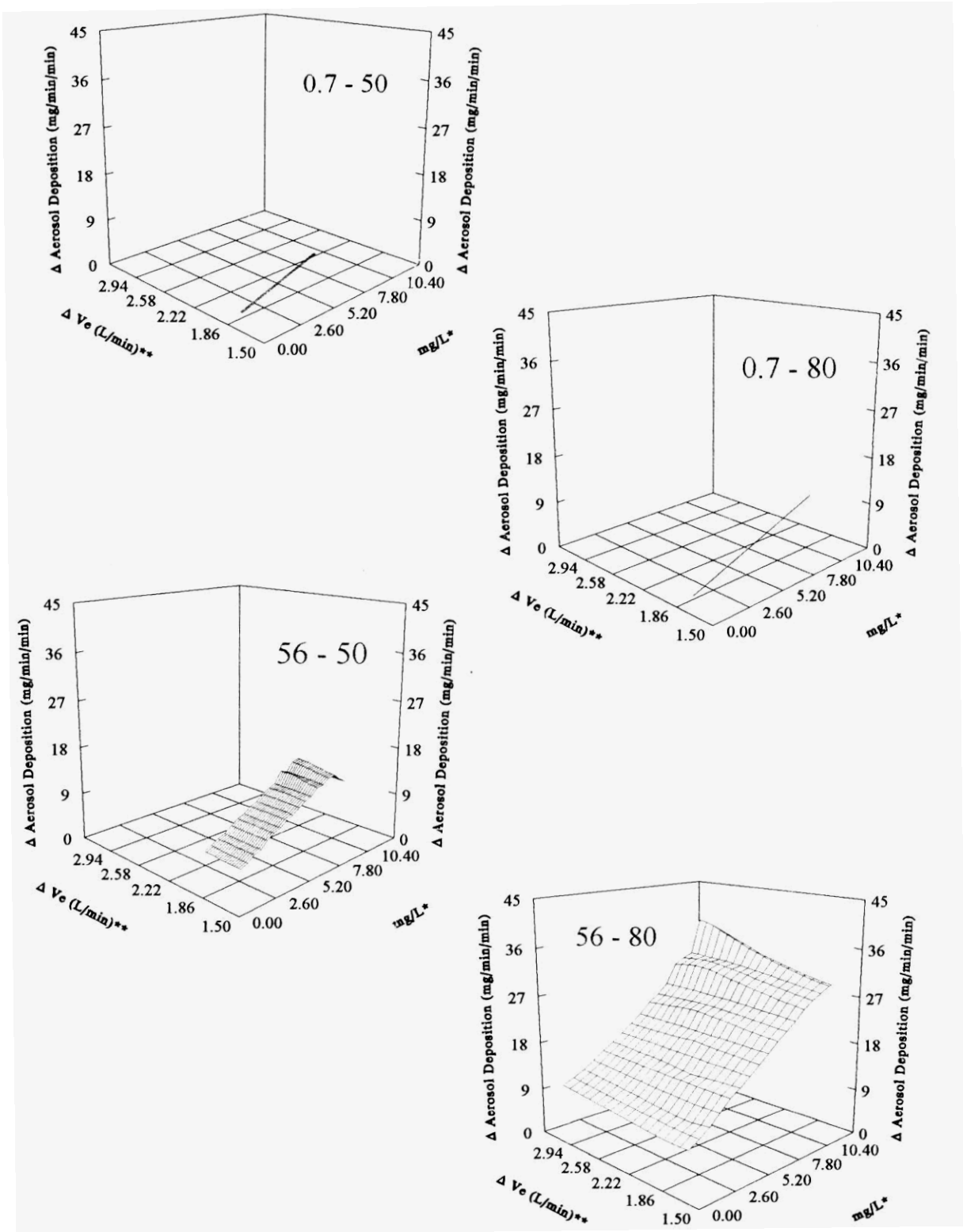


Figure 10. Increase in Particle Deposition as a Function of Aerosol Concentration and CO₂ Induced Hypercapnea
 baseline deposition = $4.9 \pm 10^{-3} \text{ g/m}^3$ from lowest concentration (0.7 g/m^3) and $V_e = 1.0 \text{ L/min}$

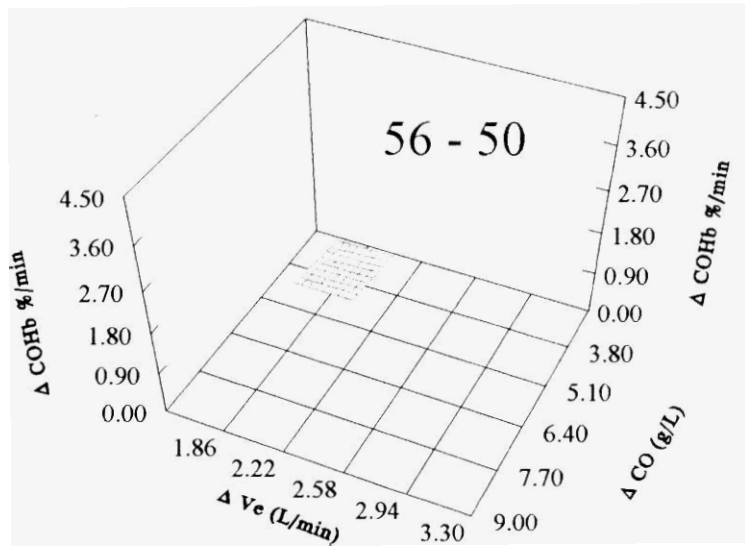
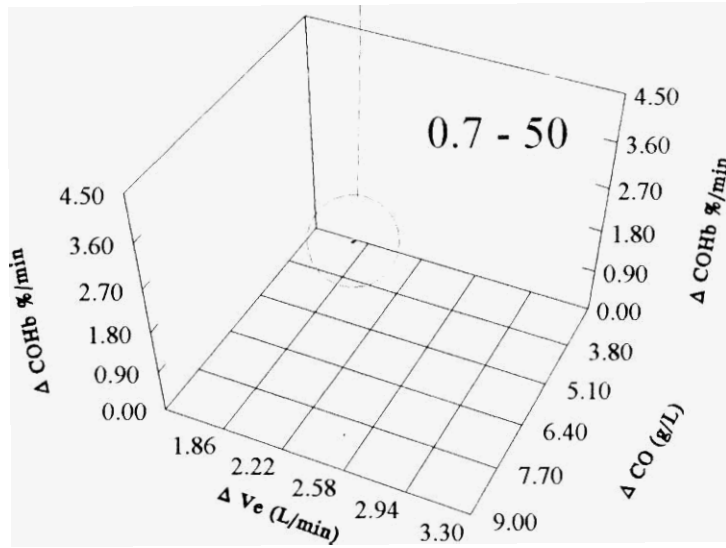
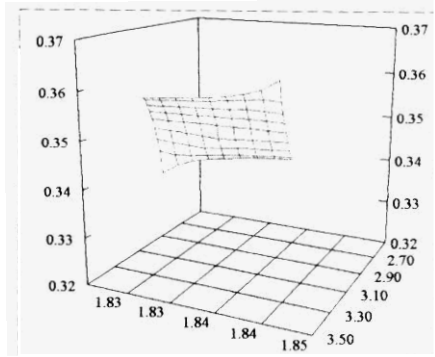


Figure 11. Carboxyhemoglobin Formation Rates

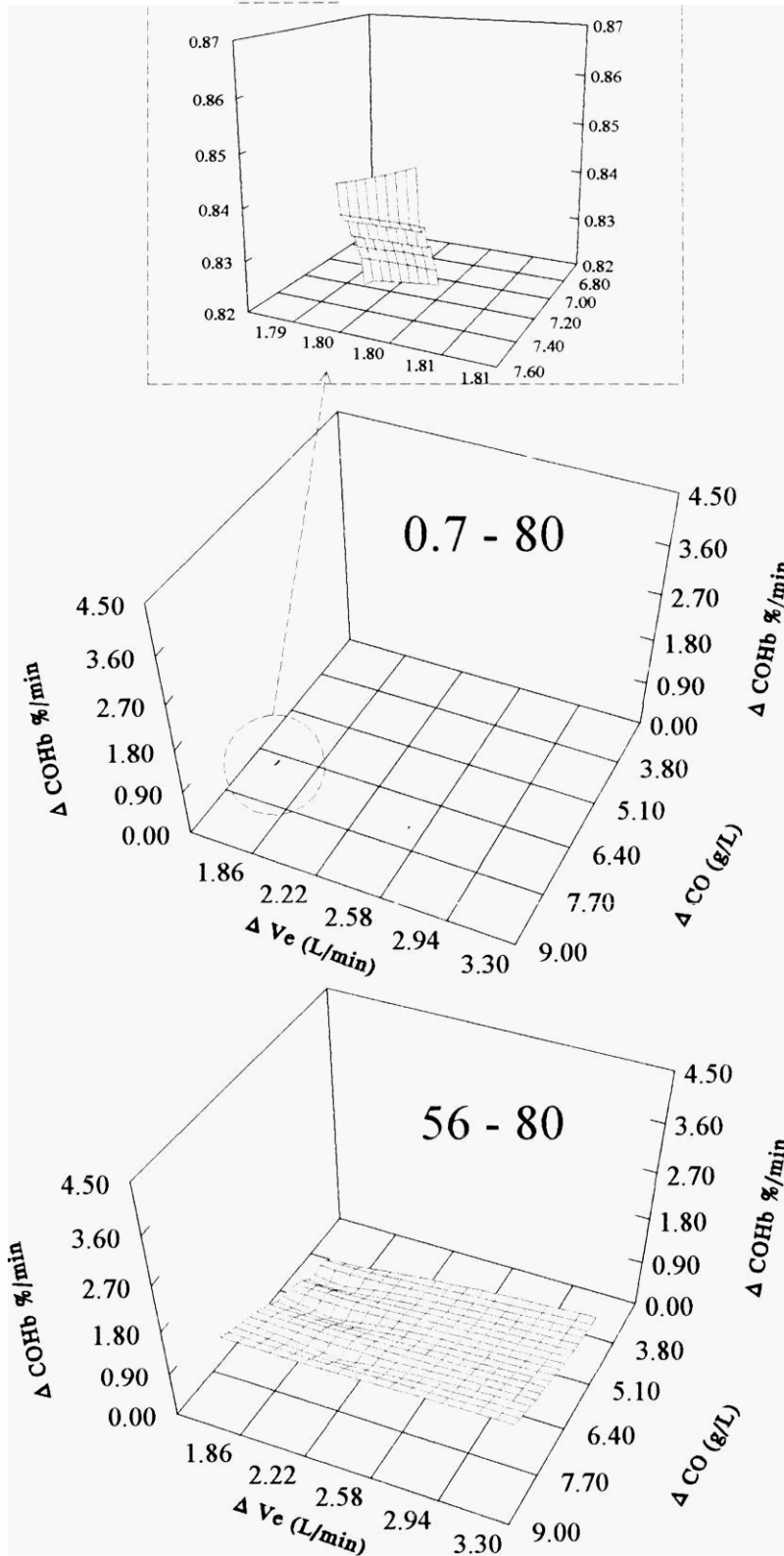


Figure 11. Carboxyhemoglobin Formation Rates